Cardiopulmonary Function in Rats With Lung Hemorrhage Induced by Pulsed Ultrasound Exposure

Jeffery M. Kramer, PhD, Tony G. Waldrop, PhD, Leon A. Frizzell, PhD, James F. Zachary, DVM, PhD, William D. O'Brien, Jr, PhD

Objective. To assess cardiopulmonary function in rats exposed to pulsed ultrasound using superthreshold exposure conditions known to produce significant lung hemorrhage. ***Methods.*** In 1 group of 9 anesthetized Sprague-Dawley rats, 5 foci of ultrasound-induced hemorrhage were produced in the left lung of each rat. In a second group of 6 rats, 5 foci of ultrasound-induced hemorrhage were produced in the left and right lungs of each rat. Each lesion was induced using superthreshold pulsed ultrasound exposure conditions (3.1-MHz center frequency, 1.7-kHz pulse repetition frequency, 1.3-microsecond pulse duration, 60-second exposure duration, 39-MPa in situ peak compressional pressure, and 17-MPa in situ peak rarefactional pressure). After exposure, the lungs were fixed in formalin and assessed histologically. The total lesion volume was calculated for each lesion in each lung lobe. Measurements of cardiopulmonary function included assessment of pulsatile arterial pressure, heart rate, end-tidal carbon dioxide, respiratory rate, and arterial blood gases (P_{CO_2} and P_{O_2}). Functional data were quantified before (baseline) and 30 minutes after exposure to ultrasound. ***Results.*** In the 9 rats that had lesions in only the left lung, the mean (SEM) lesion volume was 97 (13) mm^3 and represented about 3.4% of the total lung volume. In the 6 rats that had lesions in both the left and right lungs, the left, right, and total mean lesion volumes, respectively, were 102 (16), 114 (11), and 216 (18) mm^3 and represented about 3.7%, 4.2%, and 7.9% of the total lung volume. There were no statistically significant differences in cardiopulmonary measurements between baseline values and values obtained after exposure to ultrasound in the 9 rats exposed on the left lung only. The 6 rats exposed bilaterally had statistically significant differences in arterial pressure (134 ± 4 versus 113 ± 9 mm Hg; $P = .047$) and arterial P_{O_2} (70 ± 5 versus 58 ± 4 mm Hg; $P = .024$) between baseline values and values obtained after exposure to ultrasound. ***Conclusions.*** The severity of ultrasound-induced lesions produced in 1 lung did not affect measurements of cardiopulmonary function because of the functional respiratory reserve in the unexposed lung. However, when both the left and right lungs had ultrasound-induced lesions, the functional respiratory reserve was decreased to a point at which rats were unable to maintain systemic arterial pressure or resting levels of arterial P_{O_2}. ***Key words:*** ultrasound bioeffects; rat lung function; pulsed ultrasound; lung hemorrhage.

Abbreviations
MI, mechanical index

Received February 1, 2001, from the Department of Molecular and Integrative Physiology (J.M.K., T.G.W.), Bioacoustics Research Laboratory, Department of Electrical and Computer Engineering (L.A.F., W.D.O.), and Department of Veterinary Pathobiology (J.F.Z.), University of Illinois at Urbana-Champaign, Urbana, Illinois. Revision requested March 26, 2001. Revised manuscript accepted for publication April 18, 2001.

We thank our valued colleagues J. Blue, R. Miller, K. Norrell, and B. Zierfuss for technical contributions and E. Plowey for help with the animal preparations. This work was supported by National Institutes of Health training fellowship NIH T32GM07143 (to J.M.K.) and National Institutes of Health grant HL58218 (to W.D.O. and J.F.Z.).

Address correspondence and reprint requests to William D. O'Brien, Jr, PhD, Bioacoustics Research Laboratory, Department of Electrical and Computer Engineering, University of Illinois at Urbana-Champaign, 405 N Mathews, Urbana, IL 61801.

Patients, human or veterinary, with trauma to the lungs, pulmonary hemorrhage, or both have abnormalities of pulmonary function.[1,2] The degree of abnormal function is dependent on the severity of injury and the proportion of total lung volume damaged. Because of the very large reserve volume of the lungs, which is required during exhaustive exercise, patients can accommodate rather severe lung damage and still survive. There exists abundant published scientific literature that clearly and convincingly documents that ultrasound at commercial diagnostic levels can produce lung damage and hemorrhage in a variety of mammalian species.[3–22] The degree to which this is a medically significant problem in humans is not known.

To our knowledge, no studies have evaluated whether ultrasound-induced lung damage affects lung function, but there have been suggestions by professional bodies[17,18] that the output level from diagnostic ultrasound equipment should be kept as low as possible, particularly for neonatal exposure, because diagnostic ultrasound levels can produce hemorrhage in lung tissue in small animals. Thus, the relationship between structural and functional ultrasound-induced alterations needs to be investigated to more appropriately gauge the potential risk of ultrasound-based diagnostic techniques. Therefore, the objective of this study was to assess the effect on cardiopulmonary function in rats with lung hemorrhage induced by superthreshold ultrasound exposure—that is, exposure levels that are known to produce significant lung lesions.

Materials and Methods

Exposimetry

The exposimetry and calibration procedures have been described in detail previously.[21] Ultrasound exposure was conducted using 1 focused 51-mm-diameter lithium niobate ultrasonic transducer (ValpeyFisher Corporation, Hopkinton, MA). Water-based (distilled water, 22°C) pulse-echo ultrasonic field distribution measurements were performed according to established procedures[23] and yielded a center frequency of 3.1 MHz, a fractional bandwidth of 15%, a focal length of 56 mm, a –6-dB focal beam width of 610 µm, and a –6-dB depth of focus of 5.9 mm.

An automated procedure described previously was used routinely to calibrate the ultrasonic fields.[21,24,25] The procedure was based on the American Institute of Ultrasound in Medicine–National Electrical Manufacturers Association *Acoustic Output Measurement Standard for Diagnostic Ultrasound Equipment*[26] and the *Standard for the Real-Time Display of Thermal and Mechanical Acoustic Output Indices on Diagnostic Ultrasound Equipment*,[27] commonly referred to as the output display standard. The source transducer was mounted in a water tank (degassed water, 22°C), and its drive voltage was supplied by a RAM-5000 ultrasonic system (Ritec Inc, Warwick, RI) that had the capability to deliver up to a 5-kW single-cycle pulse into a 50-Ω load (Fig. 1). Calibrations were performed with a polyvinylidene difluoride–calibrated hydrophone (Y-34-6543; Marconi, Chelmsford, England). The in situ peak rarefactional pressure at the pleural surface was 17 MPa, and the in situ peak compressional pressure was 39 MPa. The in situ pressure values were estimated from a mean (SD) measured in vitro peak rarefactional pressure of 20.1 (1.0) MPa (n = 14), a measured in vitro peak compressional pressure of 45.7 (2.8) MPa (n = 14), and an intercostal tissue attenuation coefficient of 2.9 dB/cm at 3.1 MHz.[28] For comparison with a quantity that appears on the display of diagnostic ultrasonographic equipment, the mechanical index (MI) was 5.8. These exposure quantities were known to be superthreshold values on the basis of previous studies.[19,21,22] The purpose for providing the MI is because it is a regulated quantity[29] of diagnostic ultrasonography systems, and its magnitude is available to system operators. Thus, there is value in providing the MI to give general guidance to manufacturers and operators as to the levels we used in this study.

Animals

The experimental protocol was approved by the campus Laboratory Animal Care Advisory Committee and satisfied all University of Illinois and National Institutes of Health rules for the humane use of laboratory animals. Animals were housed in an American Association for the Accreditation of Laboratory Animal Care–approved animal facility, placed in groups of 3 or 4 in polycarbonate cages with Beta-Chip bedding (Northeastern Products, Inc, Warrensburg, NY) and wire bar lids, and provided food and water ad libitum.

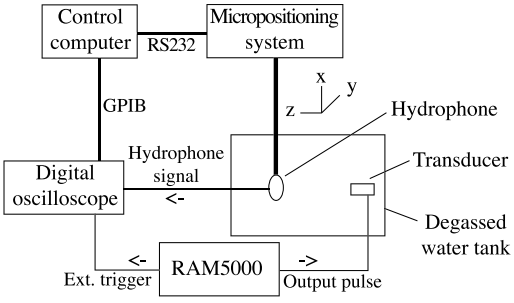

Figure 1. Block diagram of ultrasound calibration procedure.

Female Sprague Dawley rats (Harlan, Indianapolis, IN; mean [SEM], 249 [6.4] g; n = 15) were initially anesthetized with an intraperitoneal injection of α-chloralose (65 mg/kg) and urethane (800 mg/kg). A polyethylene cannula (PE-10; Clay Adams, Franklin Lakes, NJ) was subsequently placed into the right external jugular vein through a ventral midline incision in the neck for injection of supplemental anesthetic. Additional doses of anesthetic were delivered on evidence of foot withdrawal to a noxious paw pinch. A second cannula (PE-50) was placed into a common carotid artery to measure pulsatile arterial pressure using a micropressure transducer (P23; Gould, Cleveland, OH) and to sample arterial blood. Heart rate was derived from the pressure waves with the use of a biotachometer (13-4615-66; Gould). Tracheotomies were performed, and animals were allowed to spontaneously breathe room air for the duration of the experiment. Body temperature was measured with a rectal probe (Series 400; YSI Incorporated, Yellow Springs, OH) and maintained between 36.5°C and 38.0°C with the use of a heating pad and radiant heat lamp. In some cases, respiratory frequency was obtained by placing 2 stainless steel wires (A-M Systems, Carlsborg, WA) into the diaphragm and recording diaphragmatic electromyographic activity. The diaphragmatic electromyographic signal was amplified (Gould P511 differential amplifier), filtered, integrated (Gould integrator), and sent to a biotachometer to measure respiratory frequency. In other cases, respiratory frequency was obtained by measuring the interbreath interval from an end-tidal carbon dioxide measurement obtained during the experimental procedures (microcapnometer; Columbus Instruments, Columbus, OH). End-tidal P_{CO_2} measurements were obtained by placing a microsampler tip attached to the microcapnometer directly in front of the tracheotomy tube for no less than 15 breaths. The end-tidal P_{CO_2} was denoted as the peak P_{CO_2} measurement per breath averaged over 10 breaths.

Rats were allowed to acclimate under anesthesia after surgery for approximately 15 minutes, during which time they were shaved for either one- or two-sided ultrasound lung exposure. For each rat, the skin of the left side of the thorax for one-sided exposure and the left and right sides of the thorax for bilateral exposure was shaved by removing the hair with an electric clipper, followed by a depilatory agent (Nair; Carter-Wallace, Inc, New York, NY) to maximize sound transmission. Black dots were placed on the skin over the intercostal spaces between the fourth and ninth ribs to guide the positioning of the ultrasonic beam. Rats were then gently placed in the prone position, and baseline cardiorespiratory data were obtained for 2 minutes. Cardiovascular data included pulsatile arterial pressure and heart rate. Respiratory measurements included end-tidal carbon dioxide and respiratory rate. After the 2 minutes, arterial blood gas samples (500 μL) were obtained and analyzed (P_{CO_2} and P_{O_2}) with a blood gas analyzer (model 1620; Instrumentation Laboratory Company, Lexington, MA). Because of technical difficulties, arterial P_{CO_2} levels were only obtained in the two-sided lung lesion group.

Experimental Protocol

To determine the functional implications of ultrasound-induced lung damage, 2 experiments were performed. In the first experiment, only the left lung was exposed to pulsed ultrasound (n = 9), whereas in the second experiment, both the left and right lungs were exposed to pulsed ultrasound (n = 6).

Anesthetized rats were placed in right lateral recumbency, and a standoff tank was positioned in contact with the skin (Fig. 2). The transducer holder was aligned with the first, most cranial, black dot. The transducer was then placed in the standoff tank, which contained degassed water at 30°C. The low-power (in vitro peak rarefactional pressure, 0.4 MPa; in situ peak rarefactional pressure, 0.3 MPa; in vitro peak compressional pressure, 0.5 MPa; in situ peak compressional pressure, 0.4 MPa; pulse repetition frequency, 10 Hz; and MI, 0.12) pulse-echo

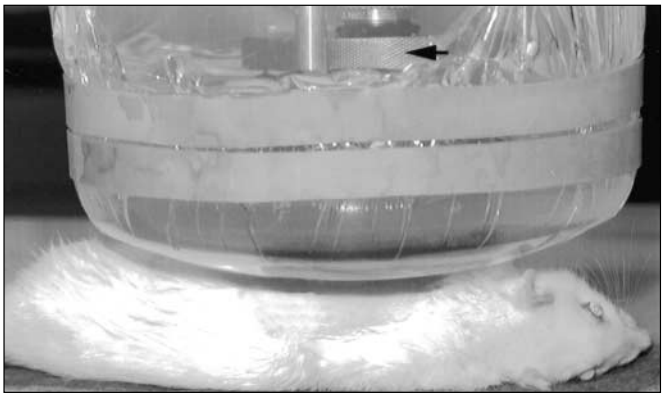

Figure 2. Rats were placed in lateral recumbancy for exposure. The 3.1-MHz ultrasonic transducer (arrow) in the standoff vessel was aligned on the lung through the intercostal spaces between the ribs.

capability of the exposure system (Ritec RAM-5000) displayed on an oscilloscope was used to adjust the axial center of the focal region to within 1 mm of the lung surface. Thus, the ultrasonic beam was approximately perpendicular to the skin at the position of the black dot, with the beam's focal region at the lateral surface of the lung. The rat was subsequently exposed. Without removing the transducer, alignment of the second, third, and fifth black dots was accomplished by moving the transducer caudally and using the Ritec system's low-power pulse-echo display capability to axially position the focal region. Alignment of the fourth black dot was accomplished identically to that of the first. The procedure was repeated with the rats in right lateral recumbency for those rats exposed bilaterally.

For each rat, 5 separate ultrasound-induced lesions were produced on the left lung for the first experiment and on both the left and right lungs for the second experiment. Each lesion was induced using superthreshold pulsed ultrasound exposure conditions (3.1-MHz center frequency, 1.7-kHz pulse repetition frequency, 1.3-microsecond pulse duration, 60-second exposure duration, 39-MPa in situ peak compressional pressure, and 17-MPa in situ peak rarefactional pressure). The in situ (at the pleural surface) acoustic intensities were determined for the measured chest wall thickness (see "Histologic Measurements") and the calibrated water-based values (45.8-MPa in vitro peak compressional pressure and 20.2-MPa in vitro peak rarefactional pressure).

Approximately 30 minutes after lung exposure, animals were returned to a prone body position, and cardiopulmonary data were obtained for 2 minutes. After the postultrasound measurements, a brief (30-second) bout of hypoxic (10% O_2 and 90% N_2) gas was delivered across the tracheotomy tube to act as a positive control for the ability of an experimental stimulus to change both arterial blood gases and cardiorespiratory function.

Histologic Measurements

After the acquisition of the cardiopulmonary data, rats were killed under anesthesia by cervical dislocation. The thorax was opened, and the thickness of the thoracic wall (skin, rib cage, and parietal pleura) at the point of the third exposure was measured using a digital micrometer (accuracy, 10 µm). These chest wall measurements were used for later calculation of the in situ ultrasonic pressures at the visceral pleural surface. The presence or absence of ultrasound-induced lung hemorrhage was recorded immediately after death. Lungs were then fixed for a minimum of 24 hours in 10% neutral-buffered formalin. After fixation, the elliptical dimensions of the lesions at the visceral pleural surface were measured with a digital micrometer (accuracy, 10 µm), where a was the length of the semimajor axis, b was the length of the semiminor axis, and d was the depth. In animals in which the depth of the lesion was not visually discernable, the depth was determined from measurements made on histologic sections with a slide micrometer. The surface area (πab) and volume ($\pi abd/3$) of the lesion were calculated for each animal assuming the lesion shape was that of a right elliptical cone, as has previously been shown in both mice and rats.[21] The volume of individually identified lesions was estimated from the surface area and depth as described. In some cases, the lesions overlapped such that the individual lesion boundaries could not be identified; thus the lesion area of the overlapping lesions was estimated from measurements of the semimajor and semiminor axes, again assuming an elliptical shape. For the overlapping lesions, the lesion depth for each overlapping lesion was estimated to be the deepest extension of each overlapping lesion. The volume of the overlapping lesions was then estimated using $\pi abd/3$. This procedure to estimate the volume of overlapping lesions would underestimate the volume, because the assumed volume geometry is a single right elliptical cone, whereas the actual vol-

ume of overlapping lesions is more likely that of the sum of the individual right elliptical cones. The lesion volume of each lung was then calculated from the sum of each of the lesion volumes of that lung. Each half of the bisected lesion was embedded in paraffin, sectioned at 5 µm, stained with hematoxylin and eosin, and evaluated microscopically.

Statistical Analysis

Lesion size data were compared with a single-factor analysis of variance (individual lung lesion area and volume). Cardiovascular and respiratory data were compared within animals by a paired Student *t* test. End-tidal carbon dioxide and arterial blood gas measurements were compared by a one-way repeated measures analysis of variance (before lung exposure, after lung exposure, and hypoxia). Individual means were compared with a Tukey post hoc analysis. All statistical tests were deemed significant at $P < .05$. All values are expressed as mean (SEM).

Results

Chest Wall Thickness

The mean thickness of the thoracic wall (skin, rib cage, and parietal pleura) at the point of the third exposure was 4.22 (0.08) mm (n = 21). This thickness value, along with previously determined chest wall insertion losses,[28] yielded 39-MPa in situ peak compressional pressure and 17-MPa in situ peak rarefactional pressure for all rat exposures.

Gross and Histologic Observations

Grossly, the lesions visible on the visceral pleural surface were red to dark red elliptical areas of hemorrhage that formed along the pathway of the ultrasound beam (Fig. 3). Examination of the bisected lesion showed hemorrhage that had a conical shape whose base opposed the visceral pleural surface and whose apex extended into subjacent lung parenchyma to varied depths within the lung. The surface area of the lesion at the pleural surface was correlated with the depth of the lesion into the subjacent lung parenchyma.[21] The microscopic lesions have been described in detail elsewhere.[21] In summary, the lesion consisted of alveolar hemorrhage without apparent injury to alveolar septa or visceral pleura. Alveoli were packed with erythrocytes and occasional accretions of plasma proteins.

Lesion Size

For the 9 rats with only the left lung exposed, the mean lesion depth was 3.1 mm (range, 1.5–4.8 mm). For the 6 rats in which both lungs were exposed, the mean lesion depths were 3.3 mm for both the left and right lungs (left range, 2.2–4.3 mm; right range, 1.8–4.9 mm). The lesion surface area and volume were slightly more than doubled between the one- and two-sided exposed lungs (mean surface areas, 81 versus 181 mm^2; mean volumes, 97 versus 216 mm^3), as graphically shown in Figure 4.

The lesion size measures were taken in the excised lung. An approximate fraction of the lung that involved a lesion was estimated from the allometric equation for wet lung weight[30]: wet lung weight (grams) = $11.3M^{0.99}$, where M is the mass of the deflated lung in kilograms. The wet lung weight was calculated for each of the 15 rats (mean lung mass, 0.249 kg; range, 0.210–0.290 kg) and yielded a mean wet lung weight of 2.85 g (range, 2.41–3.32 g). The individual wet lung weights were converted to total lung volumes by assuming a density of 1 g/cm^3, and these total lung volumes were compared with their respective lesion volumes to yield the fraction of the lung that had a lesion (Fig. 4).

Comparison of these 3 groups of lungs (9 left lungs from one-sided exposed animals, 6 left lungs from bilaterally exposed animals, and 6 right lungs from bilaterally exposed animals) did not yield statistically significant differences for lesion depth ($P = .53$), lesion volume ($P = .65$), and lesion volume fraction ($P = .59$), whereas comparison of one-sided exposed lungs with

Figure 3. Representative photomicrograph of multiple elliptical foci of hemorrhage produced in rat lung after exposure to superthreshold pulsed ultrasound. Scale bar indicates 5 mm.

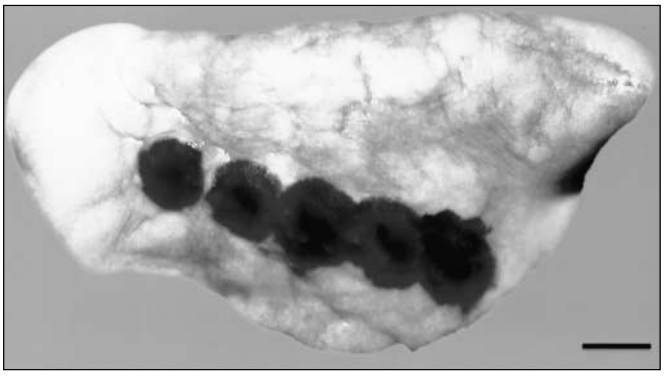

bilaterally exposed lungs (sum of both left and right lungs) yielded statistically significant differences ($P < .0001$) for lesion depth, lesion volume, and lesion volume fraction.

Cardiopulmonary Data

One-sided ultrasound-induced lung damage had no statistically significant effect on resting mean arterial blood pressure (147 ± 4 mm Hg before versus 142 ± 4 mm Hg after), heart rate (402 ± 15 beats per minute before versus 383 ± 9 beats per minute after), or respiratory frequency (73 ± 5 breaths per minute before versus 69 ± 5 breaths per minute after) (Fig. 5). Similarly, arterial blood gases were not affected by superthreshold ultrasound exposure (Fig. 6). Arterial carbon dioxide levels, estimated through end-tidal P_{CO_2} measurements, were 43 ± 2 mm Hg before lesion formation and 44 ± 2 mm Hg after ultrasound-induced lung damage. Arterial P_{O_2} levels before lesion formation were 82 ± 6 mm Hg, and those after lesion formation were 78 ± 6 mm Hg. However, when the animals were subjected to a positive control such as systemic hypoxia, the levels of arterial P_{O_2} dropped to 44 ± 2 mm Hg ($P < .05$ versus after lesion formation).

In contrast to the one-sided ultrasound-induced lung damage, the two-sided exposures caused changes in peripheral indicators of lung function. Mean arterial pressure was significantly lower ($P < .05$) after ultrasound exposure (113 ± 9 mm Hg) than before lung exposure (134 ± 4 mm Hg) (Fig. 5). Heart rate showed a similar trend but was not statistically significant (399 ± 8 beats per minute before and 376 ± 6 beats per minute after exposure; $P < .08$). Ultrasound damage had no effect on respiratory frequency. Arterial blood gas measurements were also affected by two-sided ultrasound lung exposure (Fig. 6). Arterial P_{O_2} levels were significantly lower after exposure (57 ± 4 mm Hg) than before exposure (70 ± 5 mm Hg) (Fig. 6; $P < .03$). In contrast, arterial P_{CO_2} levels were not affected by ultrasound exposure (45 ± 4 mm Hg before versus 49 ± 4 mm Hg after). Delivering hypoxic gas to the two-sided exposed animals drove down both arterial P_{O_2} levels to 32 ± 1 mm Hg ($P < .0001$) and arterial P_{CO_2} levels to 40 ± 3 mm Hg ($P < .03$).

Figure 4. Mean lesion surface area (top), mean volume (middle), and mean fraction of lung with lesion (bottom) for the 9 one-sided exposed lungs (One-sided) and the 6 bilaterally exposed lungs. For the 6 bilaterally exposed lungs, the mean values of the left lungs (L-side), right lungs (R-side), and total (Two-sided) are shown. Error bars represent SEM (n = 9 for the one-sided; n = 6 for the two-sided).

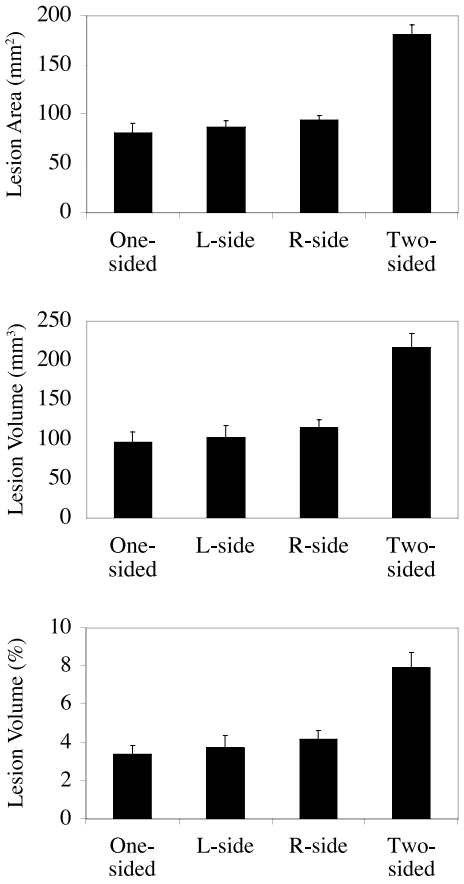

Discussion

The current findings show that in anesthetized rats, one-sided ultrasound-induced lung lesions produced no statistically significant changes in cardiovascular or respiratory function. Both systemic cardiorespiratory and blood gas measurements failed to show any peripheral indication of reduced abnormalities in lung function. However, two-sided lung exposure produced changes in both arterial blood gas measurements and cardiovascular function. Specifically, two-sided ultrasound exposure caused arterial P_{O_2} levels to drop below baseline levels 30 minutes after the end of exposure. At the same time, arterial blood pressure was significantly reduced after ultrasound exposure. In this animal prepa-

ration, reductions in arterial P_{O_2} caused decreases in arterial pressure.[31,32] The decreases in mean arterial pressure observed after two-sided exposure are consistent with the decreases in arterial P_{O_2} and help validate the arterial blood gas findings. Therefore, we conclude that two-sided ultrasound-induced lung lesions had a significant effect on blood oxygenation. This reduction in the oxygen tension of blood likely resulted from the decreased volume of functional lung tissue. This outcome does not imply that one-sided ultrasound-induced lesions did not cause impairment of function in the exposed lung tissue. Rather, we conclude that in the one-sided lung exposures, a sufficient amount of respiratory reserve was present in the unexposed lung to prevent a significant drop in arterial oxygenation. In the two-sided exposures, this was not the case.

In both the one- and two-sided ultrasound exposure models, systemic hypoxia was able to cause significant drops in arterial P_{O_2}. In the case of two-sided exposure, in which arterial P_{CO_2} measurements were also made, hypoxic hyperventilation-driven decreases in carbon dioxide tension were also noted. These positive controls show that, given a severe enough stimulus, arterial P_{O_2} can be lowered in the single lung exposure preparation. In the two-sided exposures, hypoxia caused a further drop in arterial blood oxygenation below that after the lung exposure. The latter findings suggest that ultrasound-induced decreases in arterial P_{O_2} levels did not reach a lower limit of physiologic functioning. Ultrasound exposure had no effect on respiratory frequency in either the one- or two-sided paradigm. As such, the decreases in arterial P_{O_2} after damage to both lungs were not due to a decrease in respiratory drive. Furthermore, these data suggest that the drop in arterial P_{O_2} after two-sided exposure was not sufficient to drive respiratory compensatory mechanisms such as peripheral chemoreflexes.

In both the one- and two-sided exposures, a relatively small amount of lung tissue was affected, as determined by postmortem examination (≈4% and ≈8%, respectively). Despite this relatively small volume of lung damage, the two-sided exposures still caused a significant drop in blood oxygenation. There are several potential explanations for these functional findings. First, the arterial P_{O_2} measurements were made approximately 30 minutes after the ultrasound-induced lung exposures. Given a longer recovery period, it is possible that arterial oxygen tension may have returned to prelesion control values through homeostatic reflex mechanisms. Second, we used an anesthetized animal preparation in the current set of experiments. Anesthesia is well known to suppress respiratory drive and likely contributed to the slightly lowered baseline arterial P_{O_2} levels in the current study. However, it is unknown whether the anesthetized state contributed to the significantly reduced blood oxygenation after the two-sided exposures despite the relatively low amount of total lung tissue affected. Therefore, further experiments are warranted in conscious animals to verify the current functional findings.

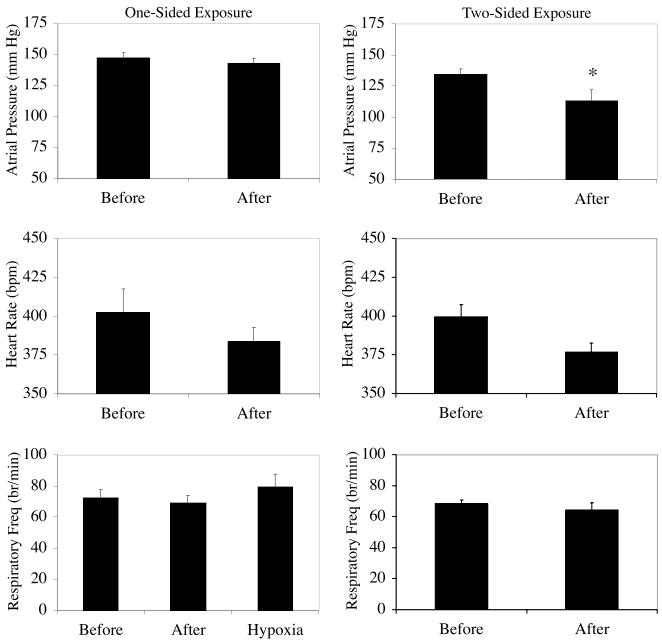

Figure 5. Cardiorespiratory (arterial pressure, heart rate, and respiratory frequency) variables measured before and after ultrasound-induced lung lesion. One-sided (left lung) lesions did not produce any significant changes in cardiorespiratory function. Two-sided (both lungs) lesions caused a significant drop in arterial pressure (*P < .05) but no change in heart rate or respiratory frequency. Error bars represent SEM (n = 9 for the one-sided; n = 6 for the two-sided).

The characteristics of the lesions produced in rats in this study were similar to those described in previous studies.[5,9,10,19–22]

The magnitude of the acoustic pressure selected for this study had to be large enough to ensure that an ultrasound-induced lesion was produced every time, and that the lesion was of a size larger than previously obtained. The in situ

Figure 6. Arterial blood gas Po_2 and end-tidal Pco_2 measurements made before and after ultrasound lung exposure. One-sided (left lung) exposure did not alter either oxygen or carbon dioxide levels; however, two-sided (both lungs) exposure significantly decreased arterial Po_2 levels in the blood (*P < .05 after versus before).

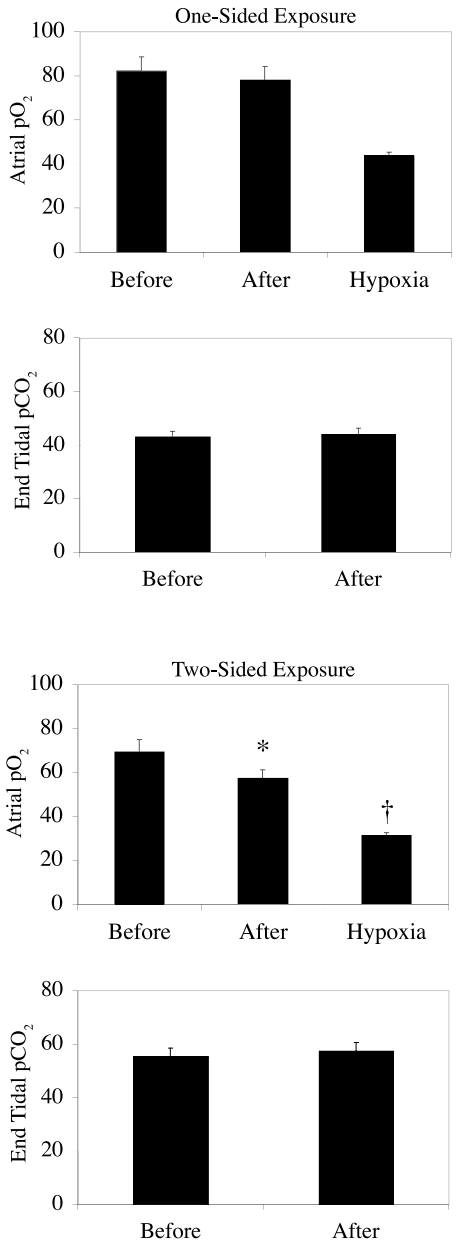

peak rarefactional pressure of 17 MPa and in situ peak compressional pressure of 39 MPa were based on our previous findings[19,21,22] in which the percentage of rats with lesions was 80% at an ultrasonic frequency of 2.8 MHz and an in situ peak rarefactional pressure of about 11 MPa. We recognize that an in situ peak rarefactional pressure of 17 MPa was considerably greater than that allowed under current regulations.[29] At this in situ peak rarefactional pressure value, the equivalent MI was 5.8, whereas the regulatory limit is 1.9 for diagnostic ultrasonic equipment that falls under FDA control.

References

1. Prentice D, Ahrens T. Pulmonary complications of trauma. Crit Care Nurs Q 1994; 17:24–33.
2. Kirton OC, DeHaven CB, Morgan JP, Windsor J, Civetta JM. Elevated imposed work of breathing masquerading as ventilator weaning intolerance. Chest 1995; 108:1021–1025.
3. Child SZ, Hartman CL, Schery LA, Carstensen EL. Lung damage from exposure to pulsed ultrasound. Ultrasound Med Biol 1990; 16:817–825.
4. Hartman C, Child SZ, Mayer R, Schenk E, Carstensen EL. Lung damage from exposure to the fields of an electrohydraulic lithotripter. Ultrasound Med Biol 1990; 16:675–679.
5. Penney DP, Schenk EA, Maltby K, Hartman-Raeman C, Child SZ, Carstensen EL. Morphologic effects of pulsed ultrasound in the lung. Ultrasound Med Biol 1993; 19:127–135.
6. Raeman CH, Child SZ, Carstensen EL. Timing of exposures in ultrasonic hemorrhage of murine lung. Ultrasound Med Biol 1993; 19:507–512.
7. Frizzell LA, Chen E, Lee C. Effects of pulsed ultrasound on the mouse neonate: hind limb paralysis and lung hemorrhage. Ultrasound Med Biol 1994; 20:53–63.
8. Holland CK, Sandstrom K, Zheng X, Rodriguey J, Roy RA. The acoustic field of a pulsed Doppler diagnostic ultrasound system near a pressure-release surface. J Acoust Soc Am 1994; 95:2855. Abstract.
9. Tarantal AF, Canfield DR. Ultrasound-induced lung hemorrhage in the monkey. Ultrasound Med Biol 1994; 20:65–72.

10. Zachary JF, O'Brien WD Jr. Lung lesion induced by continuous- and pulsed-wave (diagnostic) ultrasound in mice, rabbits, and pigs. Vet Pathol 1995; 32:43–45.

11. Baggs R, Penney DP, Cox C, et al. Thresholds for ultrasonically induced lung hemorrhage in neonatal swine. Ultrasound Med Biol 1996; 22:119–128.

12. Holland CK, Deng CX, Apfel RE, Alderman JL, Fenandez LA, Taylor KJW. Direct evidence of cavitation in vivo from diagnostic ultrasound. Ultrasound Med Biol 1996; 22:917–925.

13. Raeman CH, Child SZ, Dalecki D, Cox C, Carstensen EL. Exposure-time dependence of the threshold for ultrasonically induced murine lung hemorrhage. Ultrasound Med Biol 1996; 22:139–141.

14. Dalecki D, Child SZ, Raeman CH, Penney DP, Cox C, Carstensen EL. Age dependence of ultrasonically induced lung hemorrhage in mice. Ultrasound Med Biol 1997; 23:767–776.

15. Dalecki D, Child SZ, Raeman CH, Cox C, Carstensen EL. Ultrasonically induced lung hemorrhage in young swine. Ultrasound Med Biol 1997; 23:777– 781.

16. O'Brien WD Jr, Zachary JF. Lung damage assessment from exposure to pulsed-wave ultrasound in the rabbit, mouse, and pig. IEEE Trans Ultrason Ferroelec Freq Control 1997; 44:473–485.

17. World Federation for Ultrasound in Medicine and Biology. Symposium on Safety of Ultrasound in Medicine: issues and recommendations regarding non-thermal mechanisms for biological effects of ultrasound. Ultrasound Med Biol 1998; 24(suppl 1):S1–S55.

18. American Institute of Ultrasound in Medicine. Mechanical bioeffects from diagnostic ultrasound: AIUM consensus statements. J Ultrasound Med 2000; 19(theme issue):67–168.

19. O'Brien WD Jr, Frizzell LA, Weigel RM, Zachary JF. Ultrasound-induced lung hemorrhage is not caused by inertial cavitation. J Acoust Soc Am 2000; 108:1290–1297.

20. O'Brien WD Jr, Frizzell LA, Schaeffer DJ, Zachary JF. Superthreshold behavior of ultrasound-induced lung hemorrhage in adult mice and rats: role of pulse repetition frequency and exposure duration. Ultrasound Med Biol 2001; 27:267–277.

21. Zachary JF, Sempsrott JM, Frizzell LA, Simpson DG, O'Brien WD Jr. Superthreshold behavior and threshold estimation of ultrasound-induced lung hemorrhage in adult mice and rats. IEEE Trans Ultrason Ferroelec Freq Control 2001; 48:581–592.

22. Zachary JF, Frizzell LA, Norell KS, Blue JP Jr, Miller RJ, O'Brien WD Jr. Temporal and spatial evaluation of lesion reparative responses following superthreshold exposure of rat lung to pulsed ultrasound. Ultrasound Med Biol 2001; 27:829–839.

23. Raum K, O'Brien WD Jr. Pulse-echo field distribution measurement technique of high-frequency ultrasound sources. IEEE Trans Ultrason Ferroelec Freq Control 1997; 44:810–815.

24. Sempsrott JM, O'Brien WD Jr. Experimental verification of acoustic saturation. In: Proceedings of the 1999 IEEE Ultrasonics Symposium. Piscataway, NJ: Institute of Electrical and Electronics Engineers; 1999:1287–1290.

25. Sempsrott JM. Experimental Evaluation of Acoustic Saturation [master's thesis]. Urbana, IL: University of Illinois.

26. American Institute of Ultrasound in Medicine, National Electrical Manufacturers Association. Acoustic Output Measurement Standard for Diagnostic Ultrasound Equipment. Laurel, MD: American Institute of Ultrasound in Medicine; Rosslyn, VA: National Electrical Manufacturers Association; 1998.

27. American Institute of Ultrasound in Medicine, National Electrical Manufacturers Association. Standard for Real-Time Display of Thermal and Mechanical Acoustic Output Indices on Diagnostic Ultrasound Equipment. 1st rev ed. Laurel, MD: American Institute of Ultrasound in Medicine; Rosslyn, VA: National Electrical Manufacturers Association; 1998.

28. Teotico GA, Miller RJ, Frizzell LA, Zachary JF, O'Brien WD Jr. Attenuation coefficient estimates of mouse and rat chest wall. IEEE Trans Ultrason Ferroelec Freq Control 2001; 48:593–601.

29. Center for Devices and Radiological Health, Food and Drug Administration. Information for Manufacturers Seeking Marketing Clearance of Diagnostic Ultrasound Systems and Transducers. Rockville, MD: Center for Devices and Radiological Health, Food and Drug Administration; 1997.

30. Boggs DF. Comparative control of respiration. In: Parent RA (ed). Comparative Biology of the Normal Lung. Vol 1. Boca Raton, FL: CRC Press; 1992: 309– 350.

31. Dillon GH, Welsh DE, Waldrop TG. Modulation of respiratory reflexes by an excitatory amino acid mechanism in the ventrolateral medulla. Respir Physiol 1991; 85:55–72.

32. Nolan PC, Waldrop TG. In vivo and in vitro responses of neurons in the ventrolateral medulla to hypoxia. Brain Res 1993; 630:101–114.